

Magnitudes and Chemical Consequences of R₃N⁺-C-H···O=C Hydrogen Bonding

Carina E. Cannizzaro and K. N. Houk*

Contribution from the Department of Chemistry and Biochemistry, University of California,
Los Angeles, California 90095-1569

Received October 24, 2001. Revised Manuscript Received March 5, 2002

Abstract: The magnitude of the stabilizing interaction between an aliphatic C-H bond attached to an ammonium nitrogen and a carbonyl oxygen was evaluated by *ab initio* calculations at the MP2/6-311++G** level of theory. Attractive R₃N⁺-C-H···O=C interactions play an important role in supramolecular recognition and various types of stereoselective catalysis. Our calculations show that R₃N⁺-C-H···O=C is the strongest hydrogen bond of the C-H···O type known to date. Such hydrogen bonds remain as stabilizing interactions even in water for amide acceptors.

Introduction

In the past decade a growing interest in unusual hydrogen bonding patterns emerged in the fields of structural chemistry and biology.¹ The role of C-H···O hydrogen bonds in conformational analysis,² protein structure³ and crystal packing,⁴ molecular recognition processes,⁵ the stabilization of inclusion complexes,⁶ and in the stability and possibly even in the activity of biological macromolecules⁷ has been well documented.

The geometries of C-H···O interactions in crystal structures have been analyzed in detail.⁸ Calculated interaction energies

for different combinations of donors and acceptors in vacuum range from 0.5 to 3.8 kcal/mol,⁹ values which are approximately half the interaction energies calculated for normal nonionic O-H···O hydrogen bonds (3–8 kcal/mol^{1c}). The ability of the C-H group to donate hydrogen bonds increases with the greater s character of the hybridization of the C-H bond orbital and with the number and strength of electron-withdrawing groups on carbon.¹⁰ The electron-withdrawing ability and positive charge of ammonium ion led to high computed interaction energies in the gas phase of around 9 kcal/mol for the complex H₃N⁺-CH₃···OH₂.^{9c}

Recently, interaction energies of 88.1 kcal/mol in the gas phase were calculated for the ion pair *N*-methylpyridinium cation/dimethyl phosphate anion, a model system for the binding of pyridinium derivatives to DNA.¹¹ This strong Coulombic attraction energy drops to -19.7 kcal/mol in CHCl₃ and becomes repulsive in H₂O (+4.2 kcal/mol) for the gas-phase geometry.

We have shown that attractive interactions between trimethylammonium cation and an ester carbonyl substituent of a reacting enolate direct the stereoselective outcome of the Merck process used for the synthesis of arylpropionic acid nonsteroidal anti-inflammatory drugs (NSAIDs).¹² Sanders and co-workers¹³

* Corresponding author. E-mail: houk@chem.ucla.edu.

- (1) (a) Green, R. D. *Hydrogen Bonding by C-H Groups*; Macmillan: London, UK, 1974. (b) Desiraju, G. R. *Acc. Chem. Res.* **1991**, *24*, 290. (c) Jeffrey, G. A.; Saenger, W. *Hydrogen Bonding in Biological Structures*; Springer: Berlin, Germany, 1991. (d) Desiraju, G. R. *Acc. Chem. Res.* **1996**, *29*, 441. (e) Bernstein, J.; Etter, M. C.; Leiserowitz, L. *Structure Correlation*; Bürgi, H.-B., Dunitz, J. D., Eds.; VCH: Weinheim, Germany, 1994; Vol. 2, p 431. (f) Steiner, T. *Crystallogr. Rev.* **1996**, *6*, 1. (g) Allen, F.; Lommerse, J. P. M.; Hoy, V. J.; Howard, J. A. K.; Desiraju, G. R. *Acta Crystallogr., Sect. B* **1996**, *52*, 734. (h) Jeffrey, G. A. *An Introduction to Hydrogen Bonding*; Oxford University Press: Oxford, UK, 1997. (i) Desiraju, G. R.; Steiner, T. *The Weak Hydrogen Bond in Structural Chemistry and Biology*; Oxford University Press: Oxford, UK, 1999.
- (2) (a) Satonaka, H.; Abe, K.; Hirota, M. *Bull. Chem. Soc. Jpn.* **1988**, *61*, 2031. (b) Seiler, P.; Dunitz, J. D. *Helv. Chim. Acta* **1989**, *72*, 1125. (c) Chao, I.; Chen, J.-C. *Angew. Chem.* **1996**, *108*, 200. (d) Müller, G.; Lutz, M.; Harder, S. *Acta Crystallogr., Sect. B* **1996**, *52*, 1014. (e) Steiner, T. *J. Phys. Chem. A* **2000**, *104*, 433.
- (3) (a) Derewenda, Z. S.; Derewenda, U.; Kobos, P. M. *J. Mol. Biol.* **1994**, *241*, 83. (b) Derewenda, Z. S.; Lee, L.; Derewenda, U. *J. Mol. Biol.* **1995**, *252*, 248. (c) Bella, J.; Berman, H. M. *J. Mol. Biol.* **1996**, *264*, 734. (d) Fabiola, G. F.; Krishnaswamy, S.; Nagarajan, V.; Pattabhi, V. *Acta Crystallogr., Sect. D* **1997**, *53*, 316. (e) Chakrabarti, P.; Chakrabarti, S. *J. Mol. Biol.* **1998**, *284*, 867.
- (4) Berkovitch-Yellin, Z.; Leiserowitz, L. *Acta Crystallogr., Sect. B* **1984**, *40*, 159.
- (5) (a) Shimon, L. J. W.; Vaida, M.; Addadi, L.; Lahav, M.; Leiserowitz, L. *J. Am. Chem. Soc.* **1990**, *112*, 6215. (b) Keegstra, E. M. D.; Spek, A. L.; Zwicker, J. W.; Jenneskens, L. W. *J. Chem. Soc., Chem. Commun.* **1994**, 1633. (c) Desiraju, G. R. *Angew. Chem., Int. Ed. Engl.* **1995**, *34*, 2311.
- (6) (a) Golberg, I. *Acta Crystallogr., Sect. B* **1975**, *31*, 754. (b) Steiner, T.; Saenger, W. *J. Chem. Soc., Chem. Commun.* **1995**, 2087. (c) Braga, D.; Grepioni, F.; Byrne, J. J.; Wolf, A. *J. Chem. Soc., Chem. Commun.* **1995**, 125. (d) Houk, K. N.; Menzer, S.; Newton, S. P.; Raymo, R. M.; Stoddart, J. F.; Williams, D. J. *J. Am. Chem. Soc.* **1999**, *121*, 1479.
- (7) (a) Berger, I.; Egli, M.; Rich, A. *Proc. Nat. Acad. Sci. U.S.A.* **1996**, *264*, 734. (b) Leonard, G. A.; McAuly-Hecht, K.; Brown, T.; Hunter, W. N. *Acta Crystallogr., Sect. D* **1995**, *51*, 136. (c) Musah, R. A.; Jensen, G. M.; Rosenfeld, R. J.; McRee, D. E.; Goodin, D. B. *J. Am. Chem. Soc.* **1997**, *119*, 9083.
- (8) (a) Steiner, T. *Chem. Commun.* **1997**, 727. (b) Bernstein, J.; Davis, R. E.; Shimoni, L.; Chang, N.-L. *Angew. Chem., Int. Ed. Engl.* **1995**, *34*, 1555. (c) Steiner, T. *J. Chem. Soc., Perkin Trans. 2* **1995**, 1315. (d) Steiner, T.; Starikov, E. B.; Amado, A. M.; Teixeira-Dias, J. J. C. *J. Chem. Soc., Perkin Trans. 2* **1995**, 1321. (e) Gu, Y.; Kar, T.; Scheiner, S. *J. Am. Chem. Soc.* **1999**, *121*, 9411. (f) Steiner, T. *Chem. Commun.* **1999**, 313.
- (9) (a) Turi, L.; Dannenberg, J. J. *J. Phys. Chem.* **1993**, *97*, 7899. (b) Novoa, J. J.; Tarron, B.; Whangbo, M.-H.; Williams, J. M. *J. Chem. Phys.* **1991**, *95*, 5179. (c) Van Mourik, T.; Van Duijneveldt, F. B. *J. Mol. Struct. (THEOCHEM)* **1995**, *341*, 63. (d) Vargas, R.; Garza, J.; Dixon, D. A.; Hay, B. P. *J. Am. Chem. Soc.* **2000**, *122*, 4750–4755. (e) Scheiner, S.; Kar, T.; Gu, Y. *J. Biol. Chem.* **2001**, *276*, 9832.
- (10) (a) Allerhand, A.; Schleyer, P. v. R. *J. Am. Chem. Soc.* **1963**, *85*, 1715. (b) Scheiner, S.; Grabowski, S. J.; Kar, T. *J. Phys. Chem. A* **2001**, *105*, 10607.
- (11) Raymo, F. M.; Bartberger, M. D.; Houk, K. N.; Stoddart, J. F. *J. Am. Chem. Soc.* **2001**, *123*, 9264.
- (12) Cannizzaro, C. E.; Strassner, T.; Houk, K. N. *J. Am. Chem. Soc.* **2001**, *123*, 1668–2669.
- (13) Cousins, G. R. L.; Furlan, R. L. E.; Ng, Y.-F.; Redman, J. E.; Sanders, J. K. M. *Angew. Chem., Int. Ed. Engl.* **2001**, *40*, 423.

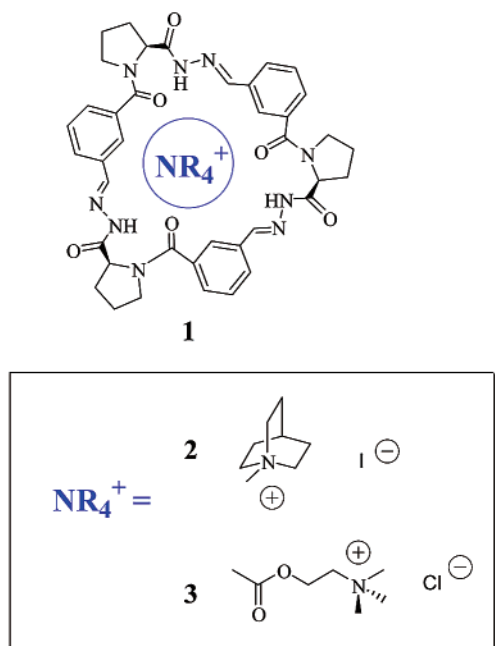


Figure 1. Ammonium recognition displayed by a dynamic combinatorial library.

have reported the identification and isolation of a new receptor for tetraalkylammonium salts based on a dynamic combinatorial chemistry (DCC)¹⁴ approach. Interestingly, the cyclic tripeptide **1** binds selectively to acetylcholine, **2**, and *N*-methylquinuclidinium salts, **3**, in chloroform ($\epsilon = 4.9$) with 1 equiv of TFA, (Figure 1). The authors believed that the driving force for templating and the 50-fold amplification of the cyclic trimer observed are the $^+N-CH_3 \cdots O=C$ hydrogen bonds between the guests and the amide moieties of the receptor. This binding rationale contrasts with that applied to other synthetic acetylcholine receptors where cation- π interactions are invoked.¹⁵

Quaternary ammonium salts of cinchona alkaloids have been extensively used in the catalysis of asymmetric reactions. Figure 2 summarizes a number of these. Cinchoninium and cinchonidinium salts have played a key role as asymmetric phase-transfer catalysts¹⁶ for a wide variety of reactions: (1) alkylation of Schiff bases of glycine¹⁷ and alanine¹⁸ esters and β,γ -unsaturated ester¹⁹ enolates with different electrophiles using **4**, (2) aldol²⁰ and nitroaldol²¹ reactions, (3) nucleophilic epoxidation of enones to give either enantiomer of epoxides²² involving **5**, (4) asymmetric Darzens reaction,²³ (5) Michael additions^{18c,24} employing **6**, and (6) asymmetric aziridination

of electron-deficient olefins by hydroxamic acids.²⁵ Purely synthetic C_2 -symmetric quaternary ammonium²⁶ and quaternary hydrazone²⁷ salts were shown to be highly efficient in the same kind of alkylation and Michael addition reactions. Finally, cinchona alkaloid derivatives, as well as other synthetic tertiary amines, have been successfully employed as chiral modifiers in the enantioselective hydrogenation of ethyl pyruvate catalyzed by platinum,²⁸ in the enantioselective dihydroxylation of olefins by osmium tetroxide,²⁹ and in the enantioselective (up to the record 87% ee) fluorination of trimethylsilyl enolates and β -cyano-esters in acetonitrile ($\epsilon = 36.7$).³⁰ In these last three cases, ammonium cations have been postulated as the reactive species, and although they are not tetraalkylammonium ions, it is possible that $^+N-CH_3 \cdots O=C$ hydrogen bonds are also important.

Although relatively nonspecific electrostatic interactions are frequently invoked for all these processes, they all possess one common feature: the formation of a relatively strong hydrogen-bonded complex between a tetraalkylammonium cation and one or more carbonyl groups of esters or amides, or the oxygen of an enolate.

We have investigated quantum mechanically the strength of these interactions in different model systems that mimic the interactions in cation-neutral carbonyl complexes and ion pairs. We selected trimethylammonium cation as a model to assess both ^+N-H and $^+N-C-H$ hydrogen bond donor groups. Methyl acetate, methyl acetate enolate, and dimethylformamide were chosen as the hydrogen bond acceptors. We report the geometries and interaction energies of the [$^+N-C-H \cdots O=C$], [$^+N-H \cdots O=C$], and [$^+N-C-H \cdots O-C=C$] hydrogen bonds present in [$Me_3NH \cdot MeCOOMe$]⁺, [$Me_3NH \cdot HCONMe_2$]⁺, and [$Me_3NH \cdot CH_2COOMe$].

Computational Methodology

Hydrogen-bonded complexes between trimethylammonium cation and methyl acetate, methyl acetate enolate, and dimethylformamide were first optimized at the restricted Hartree-Fock (RHF) level of theory and fully characterized as minima by frequency analysis. Subsequent geometry optimizations were performed at the correlated second-order Møller-Plesset (MP2) level starting from the RHF geometries. The 6-311++G** basis set, including polarization and diffuse functions on all hydrogen atoms, was used throughout this study. The reported values of binding energies include zero-point energy corrections based on the RHF vibrational frequencies, scaled by a factor of 0.89.

The effect of the polarity of different solvents on the MP2 binding energies was studied by using the Polarizable Continuum Model (PCM) of Tomasi et al.³¹ with dielectric constants of 80.1 (H₂O), 33.0 (MeOH), 7.52 (THF), 4.81 (CHCl₃), and 2.38 (toluene). Solvation calculations consisted of single points at the MP2/6-311++G** level of theory on

- (14) (a) Cousins, G. R. L.; Poulsen, S.-A.; Sanders, J. K. M. *Curr. Opin. Chem. Biol.* **2000**, *4*, 270. (b) Lehn, J.-M. *Chem. Eur. J.* **1999**, *5*, 2455. (c) Klekota, B.; Miller, B. J. *Trends Biotechnol.* **1999**, *5*, 205. (d) Sanders, J. K. M. *Chem. Eur. J.* **1998**, *4*, 1378.
- (15) (a) Kubik, S. *J. Am. Chem. Soc.* **1999**, *121*, 5846–5855. (b) Kubik, S.; Goddard, R. *J. Org. Chem.* **1999**, *64*, 9475–9487.
- (16) Nelson, A. *Angew. Chem., Int. Ed. Engl.* **1999**, *38*, 1583.
- (17) (a) Corey, E. J.; Xu, F.; Noe, M. C. *J. Am. Chem. Soc.* **1997**, *119*, 12414. (b) Lygo, B.; Wainwright, P. G. *Tetrahedron Lett.* **1997**, *38*, 8595. (c) Corey, E. J.; Noe, M. C.; Xu, F. *Tetrahedron Lett.* **1998**, *39*, 5347. (d) Ooi, T.; Takeuchi, M.; Kameda, M.; Maruoka, K. *J. Am. Chem. Soc.* **2000**, *122*, 5228.
- (18) Lygo, B.; Crosby, J.; Peterson, J. A. *Tetrahedron Lett.* **1999**, *40*, 8671.
- (19) Corey, E. J.; Bo, Y.; Busch-Petersen, J. *J. Am. Chem. Soc.* **1998**, *120*, 13000.
- (20) Horikawa, M.; Busch-Petersen, J.; Corey, E. J. *Tetrahedron Lett.* **1999**, *40*, 3843.
- (21) Corey, E. J.; Zhang, F.-Y. *Angew. Chem., Int. Ed. Engl.* **1999**, *38*, 1931.
- (22) (a) Lygo, B.; Wainwright, P. G. *Tetrahedron Lett.* **1998**, *39*, 1599. (b) Corey, E. J.; Zhang, F.-Y. *Org. Lett.* **1999**, *1*, 1287.
- (23) Arai, S.; Shioiri, T. *Tetrahedron Lett.* **1998**, *39*, 1225.
- (24) Zhang, F.-Y.; Corey, E. J. *Org. Lett.* **2000**, *2*, 1097.

- (25) Aires-de-Sousa, J.; Lobo, A. M.; Prabhakar, S. *Tetrahedron Lett.* **1996**, *37*, 3183.
- (26) Ooi, T.; Kameda, M.; Maruoka, K. *J. Am. Chem. Soc.* **1999**, *121*, 6519.
- (27) Eddine, J. J.; Cherqaoui, M. *Tetrahedron: Asymmetry* **1995**, *6*, 1225.
- (28) (a) Vargas, A.; Bürgi, T.; Baiker, A. *J. Catal.* **2001**, *197*, 378–384. (b) Blaser, H. U.; Jalett, H. P.; Lottenbach, W.; Studer, M. *J. Am. Chem. Soc.* **2000**, *122*, 12675–12682. (c) For a review see: Blaser, H. U.; Jalett, H. P.; Müller, M.; Studer, M. *Catal. Today* **1997**, *37*, 441. (d) Pfaltz, A.; Heinz, T. *Top. Catal.* **1997**, *4*, 229. (e) Baiker, A. *J. Mol. Catal. A: Chem.* **1997**, *115*, 473. (f) Schwalm, O.; Weber, J.; Minder, B.; Baiker, A. *J. Mol. Struct. (THEOCHEM)* **1995**, *330*, 353–357.
- (29) For a review see: Kolb, H. C.; VanNieuwenhze, M. S.; Sharpless, K. B. *Chem. Rev.* **1994**, *94*, 2483.
- (30) (a) For a review see: Muñoz, K. *Angew. Chem., Int. Ed. Engl.* **2001**, *40*, 1653. (b) Shibata, N.; Suzuki, E.; Takeuchi, Y. *J. Am. Chem. Soc.* **2000**, *122*, 10728. (c) Cahard, D.; Audouard, C.; Plaquet, J.-C. *Org. Lett.* **2000**, *2*, 3699.

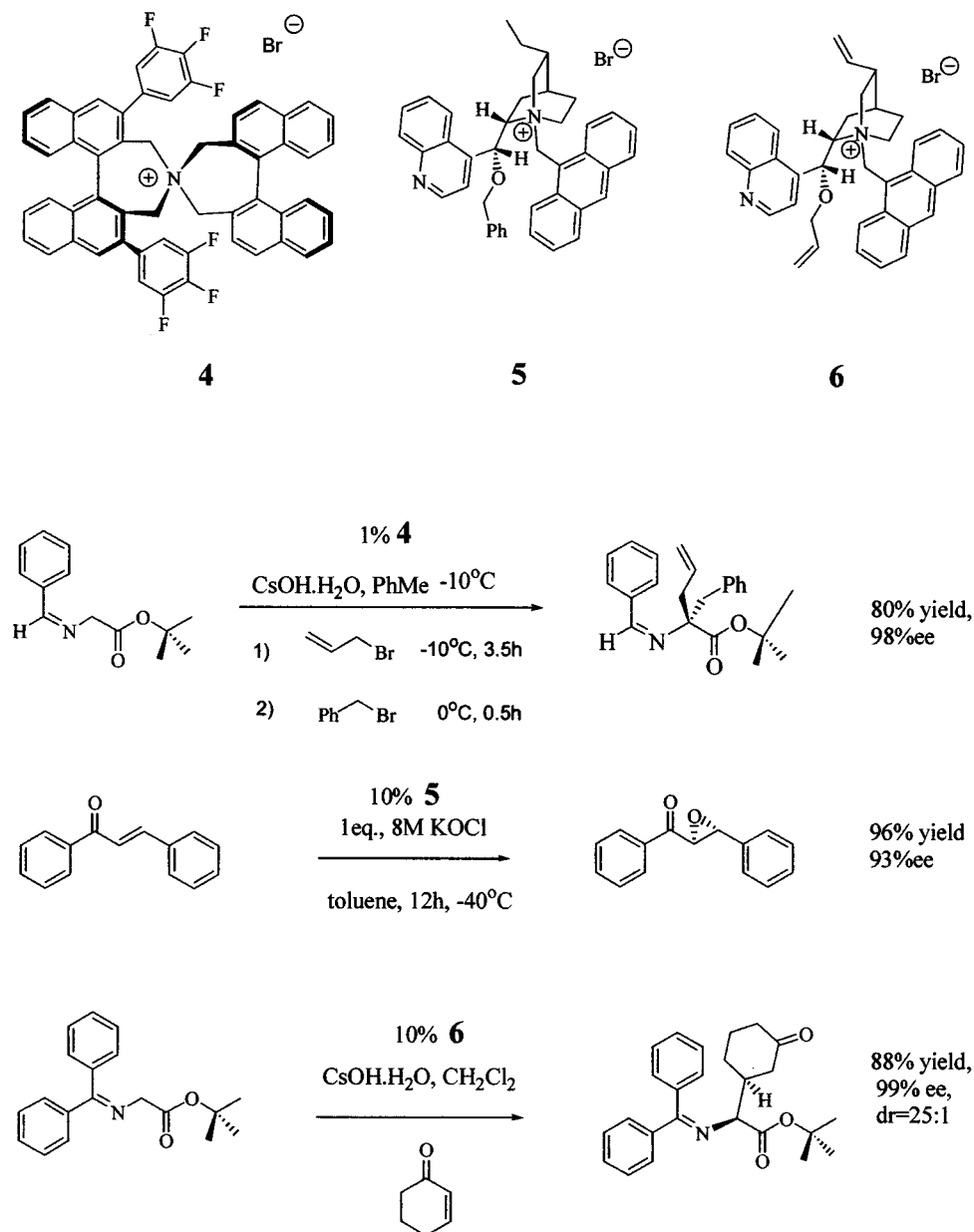


Figure 2. Chiral ammonium salts as enantioselective catalysts.

the MP2 gas-phase optimized geometries. While these calculations are still approximate because they do not include explicit solvent molecules, they do provide reasonable estimates of the effect of solvent polarity on the binding energies of the complexes. We expect a change in the geometry of the complexes upon solvation, but the size of the system and the general difficulties of convergence of the geometry optimizations involving the PCM method preclude a full optimization in solution at the MP2 level. The reported values include corrections for the basis set superposition error (BSSE) determined in the gas phase at the MP2/6-311++G** level, through the counterpoise method of Boys and Bernardi.³² All calculations were carried out with the Gaussian 98 program.³³

Electrostatic potential surfaces were created with SPARTAN.³⁴ The electrostatic potential for each structure was mapped onto a total electron density surface contour at 0.08 e/au³.

Results and Discussion

Different hydrogen-bonded complexes of Me_3^+NH with dimethylformamide or methyl acetate were constructed and

preoptimized at the RHF/6-311++G** level of theory. Those structures that corresponded to minima on the RHF/6-311++G** potential energy surface were fully optimized at the correlated level MP2/6-311++G**, giving rise to the final geometries **8**, **9**, **10**, and **11** shown in Figure 3. Similarly, the

- (31) Cossi, M.; Barone, V.; Cammi, R.; Tomasi, J. *Chem. Phys. Lett.* **1996**, *255*, 327–335.
- (32) Boys, S. F.; Bernardi, F. *Mol. Phys.* **1970**, *19*, 553–556.
- (33) Frisch, M. J.; Trucks, G. W.; Schlegel, H. B.; Scuseria, G. E.; Robb, M. A.; Cheeseman, J. R.; Zakrzewski, V. G.; Montgomery, J. A., Jr.; Stratmann, R. E.; Burant, J. C.; Dapprich, S.; Millam, J. M.; Daniels, A. D.; Kudin, K. N.; Strain, M. C.; Farkas, O.; Tomasi, J.; Barone, V.; Cossi, M.; Cammi, R.; Mennucci, B.; Pomelli, C.; Adamo, C.; Clifford, S.; Ochterski, J.; Petersson, G. A.; Ayala, P. Y.; Cui, Q.; Morokuma, K.; Malick, D. K.; Rabuck, A. D.; Raghavachari, K.; Foresman, J. B.; Cioslowski, J.; Ortiz, J. V.; Stefanov, B. B.; Liu, G.; Liashenko, A.; Piskorz, P.; Komaromi, I.; Gomperts, R.; Martin, R. L.; Fox, D. J.; Keith, T.; Al-Laham, M. A.; Peng, C. Y.; Nanayakkara, A.; Gonzalez, C.; Challacombe, M.; Gill, P. M. W.; Johnson, B. G.; Chen, W.; Wong, M. W.; Andres, J. L.; Head-Gordon, M.; Replogle, E. S.; Pople, J. A. *Gaussian 98*, revision A.7; Gaussian, Inc.: Pittsburgh, PA, 1998.
- (34) *SPARTAN SGI V5.0.3* OpenGL, 1997; Wavefunction, Inc.: 18401 Von Karman Ave., suite 370, Irvine, CA 92612.

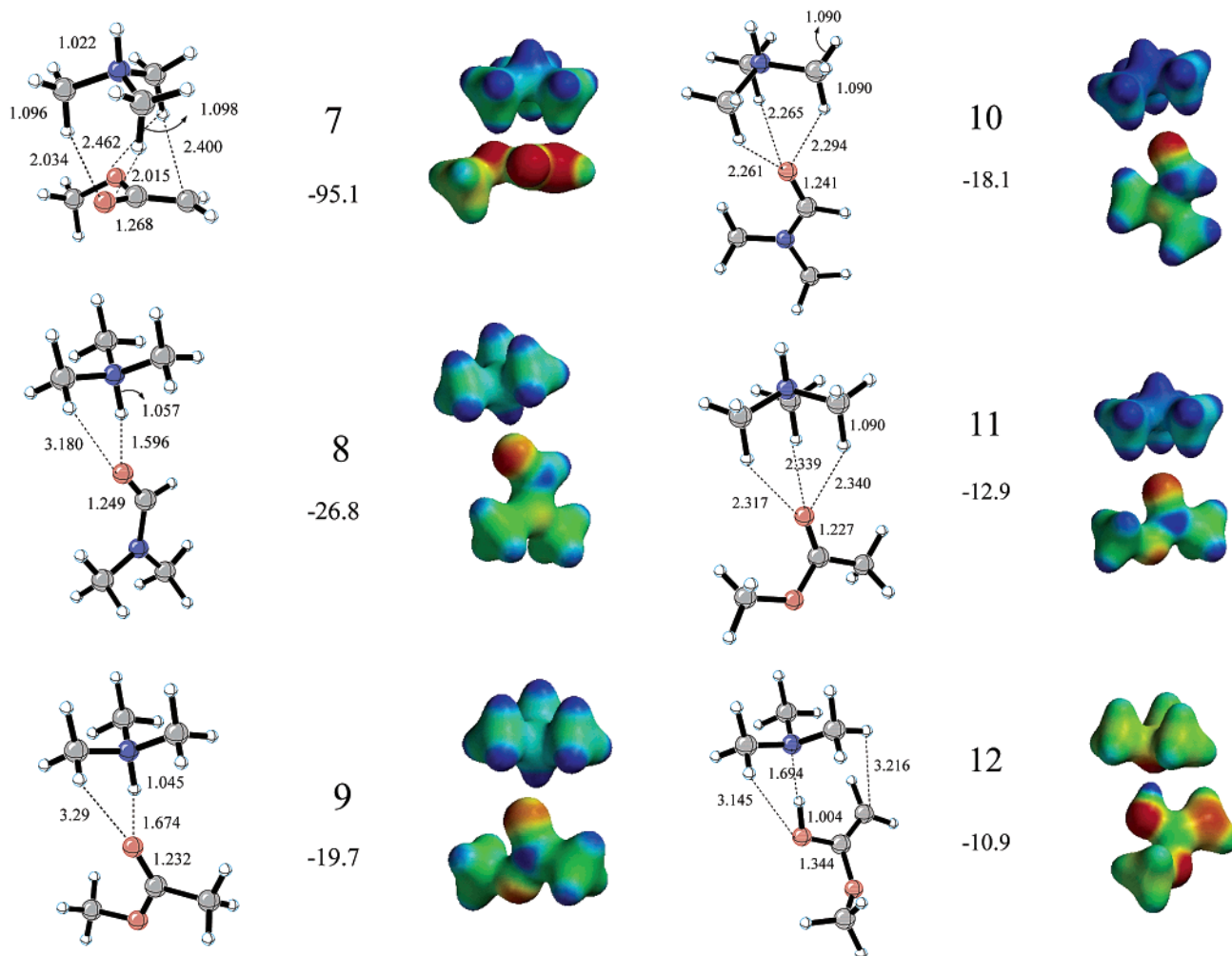


Figure 3. Computed complexes of trimethylammonium cation. Binding energies in the gas phase (kcal/mol) and electrostatic potentials are shown for each complex.

complexes between the alkoxide oxygen of methyl acetate enolate and the NH or CH protons of Me_3^+NH were preoptimized. MP2/6-311++G** optimization gave the structures **7** and **12** shown in Figure 3.

Figure 3 shows the final MP2 optimized complexes in order of decreasing stability on the left, and their corresponding electrostatic potential surfaces on the right. In **7**, the plane containing the enolate is parallel to one of the tetrahedral faces of the trimethylammonium cation. Each $\text{N}^+-\text{C}-\text{H}$ hydrogen interacts simultaneously with two of the three partially negative atoms (enolate O^- , CH_2 , and OMe) with $\text{H}\cdots\text{O}$ distances ranging from 2.015 to 2.945 Å. Five out of the six total interactions are shorter than 2.7 Å, which corresponds to the sum of the van der Waals radii of an oxygen atom (1.5 Å) and a carbon-bonded hydrogen (~ 1.2 Å).³⁵ The BSSE corrected, gas-phase MP2/6-311++G** interaction energy (Table 1) is -95.1 kcal/mol. This interaction energy is reduced to -22.2 kcal/mol in CHCl_3 , and to -40.9 kcal/mol in toluene, the most common solvents used in phase transfer catalysis, and becomes positive in water, which suggests that the stability of this ionic pair is dominated by electrostatic terms.

Corey et al.^{17a} provided a specific example of this type of interaction. They studied the X-ray crystal structures of cin-

Table 1. MP2/6-311++G** Interaction Energies for the Trimethylammonium Cation (Me_3NH^+) Complexes **7–12** and **13**^a

geometry	interaction energies (kcal/mol)					
	gas phase	toluene	CHCl_3	THF	MeOH	H_2O
7	[-97.6] -95.1	-40.9	-22.2	-15.2	$+0.7$	$+2.3$
8	[-27.5] -26.8	-16.5	-12.8	-11.3	-4.6	-3.1
9	[-20.6] -19.7	-10.3	-7.5	-6.2	$+0.3$	$+0.8$
10	[-19.0] -18.1	-9.4	-6.8	-5.5	-2.0	-1.7
11	[-14.1] -12.9	-5.2	-3.4	-2.2	$+2.0$	$+2.4$
12	[-12.8] -10.9	-8.1	-7.8	-7.2	-4.3	-3.9
13	[-8.1] -8.7	-1.6				

^a The values in square brackets correspond to the interaction energies calculated by subtracting the energies of the separately optimized and zero-point corrected donor and acceptor molecules, from the energy of the optimized and zero-point energy corrected complex [MP2/6-311++G** + ZPE(RHF)]. The other values correspond to BSSE corrected interaction energies.

chonidinium *p*-nitrophenoxide salts and formulated a model that explains the highly enantioselective alkylation of β,γ -unsaturated ester enolates. They proposed that the efficient transfer of stereochemical information between the ammonium salt and the

(35) Taylor, R.; Kennard, O. *J. Am. Chem. Soc.* **1982**, *104*, 5063–5070.

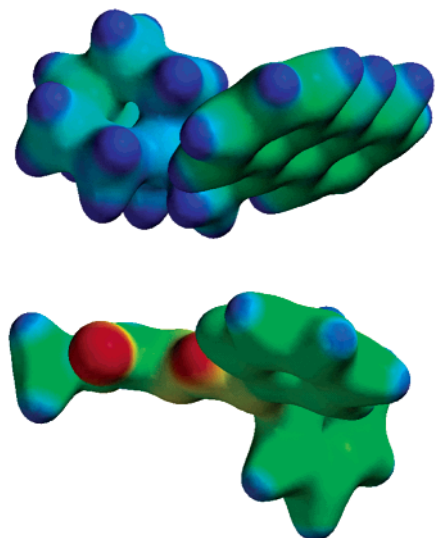


Figure 4. New model proposed for the enantioselective alkylation of *tert*-butyl glycinate-benzophenone Schiff base catalyzed by cinchonidinium salt.

enolate is possible because the quaternary ammonium structure has a well-defined geometry in which the negative oxygen of the aryloxy counterion is in close contact ($O^-\cdots N^+ = 3.46 \text{ \AA}$) with the least sterically hindered tetrahedral face of N^+ .

They assumed that the enolate oxygen forms an intimate ion pair with the cation in the same way as *p*-nitrophenoxide and developed a model that explains the enantioselectivity in which the plane of the enolate double bond is perpendicular to the plane defined by the three N^+-C-H hydrogen-bonding hydrogens. The *tert*-butyl group of the enolate is in close van der Waals contact with the *N*-9-anthracenylmethyl substituent exposing the *si* face to electrophilic attack. Our results suggest that it is the combination of three N^+-C-H interactions with the π face of the enolate that is strong enough in organic solvents to be responsible for the tight association of the reacting enolate and the ammonium catalyst. Furthermore, the optimized structure, **7**, of the complex $[Me_3NH\cdot CH_2COOMe]$ shown in Figure 3 provides the most stabilized ion pair arrangement, in which one face of the enolate is parallel to one of the four tetrahedral faces of the N^+ cation, with shorter hydrogen bond distances. The ion pair **7** in Figure 3 is the only minimum on the MP2 potential energy surface, regardless of the starting structure preoptimized at the HF/6-311++G** level. Ion pair **7** is approximately 4.3 kcal/mol more stable in the gas phase than an optimized ion pair arrangement in which only the enolate oxygen interacts with the N^+-C-H bonds (single point at the MP2 level on a fully optimized HF geometry that resembles that of structure **10**). Upon solvation this energy difference decreases to 3.0 kcal/mol in toluene and to 2.6 kcal/mol in water. The results reported here suggest an alternative model that also explains the enantioselectivity observed based on the preferred arrangement of the enolate and the cation in the highly organized transition state. In this model, the ion pair arrangement resembles that of structure **7** (Figure 3), but now the phenyl substituent of the enamine is π -stacked with the *N*-9-anthracenylmethyl substituent, exposing the *si* face to electrophilic attack. Figure 4 shows the electrostatic potential of a model of the enolate derived from *tert*-butyl glycinate-benzophenone Schiff base approaching a portion of the ammonium catalyst **6** (Figure 2). The three $C-H$ bonds α to the quaternary N are parallel to

each other, and the three hydrogens (blue in the electrostatic potential plot) define a plane. The deep blue of the N^+-C-H hydrogens corresponds to the most positive electrostatic potential on the catalyst and complements well the negatively charged positions (in red) of the reacting enolate. This arrangement also allows π stacking between the electron-rich phenyl ring of the enolate and the electron-deficient anthracenyl unit of the catalyst. When trimethylammonium interacts with neutral hydrogen bond acceptors (**8**, **9**, **10**, and **11** in Figure 3), the interaction energy in the gas phase drops significantly but is still substantial. Dimethylformamide is a better hydrogen bond acceptor, and this is reflected in the larger interaction energies of **8** and **10** with respect to **9** and **11**, respectively.

The gas-phase stabilization energy calculated for **11**, -12.9 kcal/mol, is in excellent agreement with experimental values of -12.1 ± 1.2 kcal/mol for the hydrogen-bonded complex between tetramethylammonium and methyl acetate. Pulsed high-pressure mass spectrometry was also used to evaluate the binding energies between $(CH_3)_4N^+$ and amide groups such as dimethylacetamide and methyl acetyl glycinate, and showed that they bind even more strongly (18–20 kcal/mol), in agreement with the calculated value for complex **10** (18.1 kcal/mol).³⁶

We observe a strong complementarity between the positive electrostatic potential on the $N-H$ and $C-H$ bonds of trimethylammonium (represented by the deep blue color), and the negative electrostatic potential (bright red) on the $OCOCH_2$ fragment of methyl acetate enolate of **7**, and on the carbonyl oxygen of dimethylformamide in **8** and **10** and methyl acetate in **9** and **11** (Figure 3). Similar intensity of blue on the N^+-H and the N^+-C-H bonds indicates areas of comparable electrostatic potential.

There is an increase of $C-H$ bond length from 1.090 \AA in trimethylammonium to 1.098, 1.096, and 1.095 \AA upon formation of complex **7**. Elongation of $N-H$ bonds was also observed, from 1.024 \AA in trimethylammonium to 1.057 and 1.045 \AA in complexes **8** and **9**, respectively, although no changes in $C-H$ bond length were observed for complexes **10** and **11**. Finally, the enol $O-H$ bond length increased from 0.963 in the isolated enol to 1.004 \AA in the hydrogen-bonded complex **12**. These observations correlate with the following order of hydrogen bond strength: $[N^+-C-H\cdots O=C] < [N^+-H\cdots O=C] < [N\cdots HO=C]$.

Several generalizations can be made: (1) The stabilization of the complexes **10** and **11** in the gas phase that involve three $N^+-CH_3\cdots O=C$ hydrogen bonds is two-thirds of the stabilization of complexes **8** and **9**, respectively, that involve one strong $N^+-H\cdots O=C$ hydrogen bond and two longer and weaker $N^+-CH_3\cdots O=C$ hydrogen bonds. The stabilization of the complexes **10** and **11** in solvent is half of the stabilization of complexes **8** and **9**, respectively, regardless of the polarity of the solvent. These results suggest that any process that allows these $N^+-CH_3\cdots O=C$ interactions to occur in concert will be highly stabilized, even in organic solvents of moderate to low polarity (THF, $CHCl_3$, toluene).

(2) Three $^+N-CH_3\cdots O=C$ hydrogen bonds are more effective in stabilizing the resulting hydrogen-bonded complexes (**7**, **9**, and **11**) than the strong $[N\cdots H-O]$ hydrogen bond present in structure **12**, where trimethylamine is hydrogen bonded to methyl acetate enol in the gas phase. Although these $N^+-CH_3\cdots$

(36) Deakne, C. A.; Meot-Ner, M. *J. Am. Chem. Soc.* **1999**, *121*, 1546–1557.

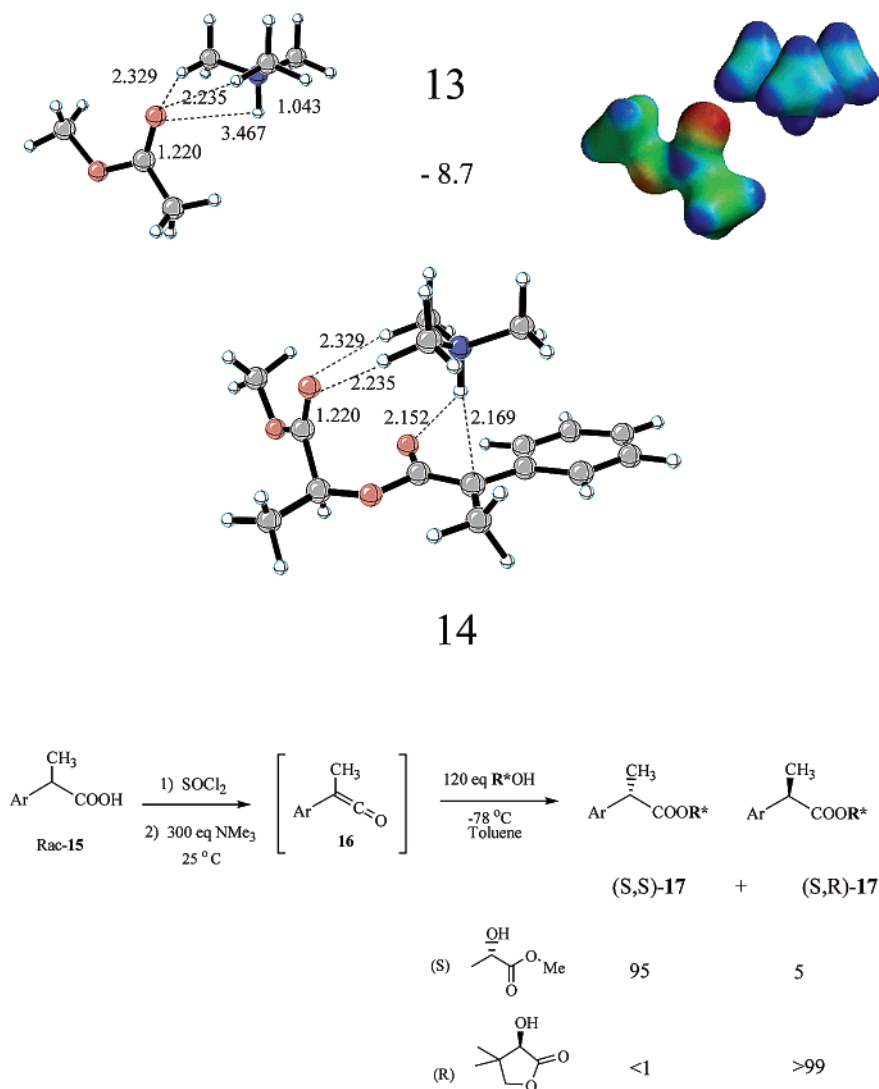


Figure 5. Model for the hydrogen bonding interactions of the enol–keto tautomerization (above); fully optimized transition state for the diastereoselectivity determining step in the Merck process.

$\cdots\text{O}=\text{C}$ hydrogen bonds are completely suppressed in water and MeOH, they remain as competitive stabilizing interactions in common organic solvents such as THF.

(3) The hydrogen-bonding interactions involving the amide carbonyl as the hydrogen bond acceptor (structures **8** and **10**) are not completely suppressed in water. This observation suggests that $[\text{N}^+-\text{C}-\text{H}\cdots\text{O}]$ interactions involving aspartate or glutamate residues or even the amide backbones of proteins could control the recognition of quaternary ammonium haptens by catalytic antibodies, and therefore be responsible for catalysis by stabilizing the cationic transition states that are mimicked by ammonium haptens. Antibody 14D9, for example, was elicited toward a piperidinium derivative that mimics the rate-limiting transition state in the pH-dependent hydrolysis of ketals³⁷ and epoxides,³⁸ as well as the transition state for the enantioselective protonation of enol ethers.³⁹ The aspartate or glutamate residues present in the active site of 14D9 proved to be the major factor in the catalytic activity.⁴⁰

Figure 5 shows a model, **13**, for the interaction between the $\text{N}^+-\text{C}-\text{H}$ bonds of the trimethylammonium catalyst and the ester carbonyl substituent of (*S*)-methyl lactate, as they interact in the transition state, **14**, of the enol–keto tautomerization step. This determines the diastereoselectivity of the Merck process for the addition of chiral alcohols to ketenes.¹² This model was constructed from the original transition state (calculated at B3LYP/6-31G*) shown below in Figure 5 by deleting the phenylmethyl ketene enolate and substituting the methyl and OH groups of the (*S*)-methyl lactate by hydrogen atoms. Only the coordinates of these newly added hydrogens were allowed to optimize at the MP2 level while the rest of the structure remained frozen, to give **13**. Two $[\text{N}^+-\text{C}-\text{H}\cdots\text{O}=\text{C}]$ hydrogen bonds are present with $\text{H}\cdots\text{O}$ distances of about 2.2–2.3 Å and

(37) Reymond, J.-L.; Janda, K. D.; Lerner, R. A. *Angew. Chem., Int. Ed. Engl.* **1991**, *30*, 1711.

(38) Sinha, S. C.; Keinan, E.; Reymond, J.-L. *J. Am. Chem. Soc.* **1993**, *115*, 4893.

(39) (a) Reymond, J.-L.; Janda, K. D.; Lerner, R. A. *J. Am. Chem. Soc.* **1992**, *114*, 2257. (b) Reymond, J.-L.; Janhangiri, G. K.; Stoudt, C.; Lerner, R. A. *J. Am. Chem. Soc.* **1993**, *115*, 3909. (c) Sinha, S. C.; Keinan, E.; Reymond, J.-L. *Proc. Natl. Acad. Sci.* **1993**, *90*, 11910. (d) Reymond, J.-L.; Reber, J.-L.; Lerner, R. A. *Angew. Chem., Int. Ed. Engl.* **1994**, *33*, 475. (e) Janhangiri, G. K.; Reymond, J.-L. *J. Am. Chem. Soc.* **1994**, *116*, 11264. (f) Shabat, D.; Itzaky, H.; Reymond, J.-L.; Keinan, E. *Nature* **1995**, *374*, 143.

(40) Shabat, D.; Sinha, S. C.; Reymond, J.-L.; Keinan, E. *Angew. Chem., Int. Ed. Engl.* **1996**, *35*, 2628–2629.

C–H–O angles of 150–152°, similar to those in the fully optimized complex **11** with $H\cdots O$ distances around 2.3 Å and C–H–O angles of 142–143°. Nevertheless, the stabilization energy decreases to about 50% in the gas phase, underlining the synergistic effect of these interactions that seems to be more important than their directionality. These hydrogen bonds, responsible for facial control of the proton delivery to the enolate carbon, are worth 1.6 kcal/mol in toluene, the solvent used in the experiments.

Conclusions

In the gas phase the stabilization of complexes involving three $[N^+-C-H\cdots O=C]$ hydrogen bonds is two-thirds of the stabilization involving one $[N^+-H\cdots O=C]$ hydrogen bond. Upon solvation, the stabilization of complexes containing $[N^+-C-H\cdots O=C]$ hydrogen bonds is only one-half the stabilization from one $[N^+-H\cdots O=C]$ hydrogen bond, regardless the polarity of the solvent. Furthermore, the $[N^+-C-H\cdots O=C]$ interaction is the strongest hydrogen bond of the type C–H \cdots O known to date for an amide carbonyl acceptor (**10** in Figure 3). Stabiliza-

tion energies are comparable to the complex between trimethylamine and an enol in the usual range of solvent polarities. The fact that they remain as stabilizing interactions in water could have implications for biological phenomena such as the recognition of the quaternary ammonium, acetylcholine, by its receptor during the transmission of nerve impulses.^{41–43}

Acknowledgment. We are grateful to the National Institute of General Medical Sciences, National Institutes of Health for financial support of this research, to the UCLA Graduate Division for a Dissertation Year Fellowship to C.E.C., and to the National Computational Science Alliance for super-computer time allocation on the Origin2000 I (Grant number MCA93S015N).

JA012417Q

-
- (41) Unwin, N. *Nature* **1995**, *373*, 37–43.
(42) Botti, S. A.; Felder, C. E.; Lifson, S.; Sussman, S.; Silman, I. *Biophys. J.* **1999**, *99*, 2430–2450.
(43) (a) Rosenberry, T. L. *Acetylcholinesterase. Adv. Enzymol. Relat. Areas Mol. Biol.* **1975**, *43*, 103–218. (b) Sussman, J. L.; Harel, M.; Frolow, F.; Oefner, C.; Goldman, A.; Toker, L.; Silman, I. *Science* **1991**, *253*, 872–879.